SUPPLEMENTARY FIGURE LEGENDS

Supplemental Figure 1. FACS analysis of HIV retroviral restriction by A3G variants.
Shown are the FACS analyses of infections that occurs at the highest viral titer examined (50 ng p24, infecting 10^5 Jurkat cells). All the viruses are NL4-3 ΔVif−ΔE-eGFP variants which were generated with the encapsidated A3G variant or no A3G as indicated.

Supplemental Figure 2. A3G loop variants mutagenize HIV.
The likelihood of a G→A transition mutation at each position in a region of the HIV *pol* gene was computed for hypermutated viral genomes recovered from infection with virus containing A3G variants. Numbering is relative to the reference strain HXB2 (HIV Sequence Locator, Los Alamos National Laboratories).

Supplemental Figure 3. Expression of AID variants.
A, Expression of AID variants in DT40 B-cells. AID constructs were stably transfected into $AID^{-/-}$ $UNG^{-/-}$ IgM^{+} DT40 cells. After 8-14 weeks in culture, IgM^{-} DT40 cells were collected from pooled transfectants and RNA was prepared. Real-time PCR analysis of mRNA expression of AID is shown, relative to β-actin expression. Results shown are from three replicates with associated standard deviation. N.D., not detected.
B, Expression of AID variants in mouse $AID^{-/-}$ splenic B cells. Constructs were introduced by retroviral infection into $AID^{-/-}$ mouse splenic B cells. Quantiative PCR analysis of mRNA expression is shown, relative to β-actin expression showing similar expression levels of AID variants. Error bars represent the standard deviation from at least three measurements. N.D., not detected.

Supplemental Figure 4. Impact of local targeting on SHM and CSR is proportionally related to *in vitro* deamination levels.
A, Mistargeting to non-CDR regions is proportional to non-hotspot targeting. *In vitro* data was derived from studies on AID181-WT, AID181-3FL and AID181-3GL previously reported (Kohli et al., 2009; Ref *27*). The average rate of targeting AID hotspots (WRC) was calculated from the reported deamination of S60-AAC + S60-AGC + S60-TAC + S60-TGC. The rate of deamination of non-WRC sequences is calculated from the average rate of deamination of all other S60-XXC substrates. Plotted is the ratio of WRC to non-WRC deamination on the left y-axis (red). The right y-axis shows CDR to non-CDR targeting taken from Table 2.
B, Switching is proportional to targeting of the AID hotspot WRC. *In vitro* data was derived from the studies as above, with the average deamination of S60-WRC substrates on the left y-axis (red). The right y-axis reproduces the amount of class switching to IgG1 observed in Fig. 4.

Supplemental Figure 5. Selection of loop grafting site in AID influences resulting activity.
A, Alignment of loop graft variants evaluated. Our initial evaluation of loop graft variants (Kohli et al., 2009; Ref *23*) grafted the entire region from 113-123 into the scaffold of maltose binding protein fused, C-terminally truncated AID (AID181-WT). The selection of the loop origin was based on the recognition of conserved flanking sequences, to generate the variant AID181-3GL. In other studies (Wang et al., 2010; Ref *25*), for A3G loop graft variants were evaluated that started at position 115. To increase activity "upmutant" version of AID had to be used which containing an additional three mutations that increased catalytic activity. A version of the AID181-3GL variant was created to mimic this shifted position grafting position (AID181-3GL I113L). To further evaluate this position an additional variant AID181-3GL I113A was evaluated.
B, Assay for shift to A3G specificity. Single stranded 27-mer DNA substrates with a central CCC motif (S27-CCC) and a 3'-fluorescein residue (FAM) were used in the assay. The substrates contained no additional cytidine residues in the rest of the sequence. 1 μM S27-CCC substrate

was incubated with 1 μM AID variant and 1 U UNG (NEB) in 20 mM Tris-Cl (pH 8.0), 30 mM NaCl, 1 mM DTT, 5 mM EDTA for 12 hrs at 30 ºC, followed by heating to 95 ºC for 20 min. Abasic sites were cleaved by the addition of an equal volume of formamide and 1/10 volume of 2 M NaOH followed by incubation at 95 ºC for 20 min. Samples were run on a 20% acrylamide/TBE/urea gel and imaged using a Typhoon variable mode imager.

C, Identity of position 113 impacts catalytic activity. Assay with the AID181 variants demonstrates that AID181-WT shown limited deamination of the A3G hotspot CCC. By contrast AID181-3GL is highly proficient at deamination of S27-CCC. The identity of the position 113 residue is significant, as I113A variant shown negligible activity and I113L is compromised for deamination. We therefore conclude that the need to evaluate "upmutant" versions of AID could have resulted from the inappropriate selection of the initial position for loop grafting.

Table S1: Oligonucleotide substrates, primers, probes and mutagenic oligonucleotides

A3G-pCDNA Forward	G CCG CTC GAG AGG atg aag cct cac ttc aga aac aca gtg gag cg
A3G-pCDNA Reverse	TTT TTG TTC GAA GTT TTC CTG ATT CTG GAG AAT GGC CCG CAG CCT
A3G-3FL Forward	GTA GTC AGT GTC CCA AAA ATA ATA CAG gcg ggc agt gaa gat gca cag gct cac gtg
A3G-3FL Reverse	gcc cgc CTG TAT TAT TTT TGG GAC ACT GAC TAC cag gag ggg ctg cgc acc ctg
A3G-AL Forward	CTG TAT TTT TGC GAA GAT CGT AAA GCT GAG CCC gag ggg ctg cgc acc ctg cgc
A3G-AL Reverse	GGG CTC AGC TTT ACG ATC TTC GCA AAA ATA CAG gcg ggc agt gaa gat gca cag gct cac
A3G-E259A Forward	GGT TTC CTT GAA GGC CGC CAT GCA GCG CTG TGC TTC CTG GAC GTG ATT CCC TTT
A3G-E259A Reverse	AAA GGG AAT CAC GTC CAG GAA GCA CAG CGC TGC ATG GCG GCC TTC AAG GAA ACC
HIV cDNA realtime FOR	TGT GTG CCC GTC TGT TGT GT
HIV cDNA realtime REV	GAG TCC TGC GTC GAG AGA GC
HIV cDNA probe	(FAM)-CAGTGGCGCCCGAACAGGGA-(BHQ)
AID-RV Forward	GGA GAC CCC TGC CTA GGG ACC ACC GAC CC
AID-RV Reverse	CCC CTA CCC GGT AGA ATT CGC GGC CGC
AID-RV-3FL Forward	TAT TTT TGG GAC ACT GAC TAC CAG gag ggg ctg cgg cgg ctg cac
AID-RV-3FL Reverse	CTG GTA GTC AGT GTC CCA AAA ATA gta gag gcg cgc ggt gaa gat cct
AID-RV-3GL Forward	ATT TAC GAC GAC CAA GGG AGG TGC CAG gag ggg ctg cgg cgg ctg cac
AID-RV-3GL Reverse	CTG GCA CCT CCC TTG GTC GTC GTA AAT gcg cgc ggt gaa gat cct cag act
AID-RV-E58A Forward	AAC GGC TGC CAC GTG GCA CTG CTC TTC CTC CGC
AID-RV-E58A Reverse	GCG GAG GAA GAG CAG TGC CAC GTG GCA GCC GTT
AID-RV Empty FOR	AAG AAG AGA CGT TGG GTT ACC TTC TGC TCT GC
AID-RV Empty REV	TAG ACG AGA ATT CGG TGG ATC TAA TTC CGG CGC CTA GAG AAG GAG
S27-CCC-FAM	AGA ATT AAG TTA CCC TAG TTA AGT TAT –(FAM)
HIV Pol FOR A	GAA AGG ATC ACC AGC AAT ATT CCA GTG TAG C
HIV PolVif A REV A	CTT TAT CTG TTT TGG TTT TAT TAA TGC TGC TAG TGC
HIV Pol FOR B	aa gaa ttc ATC TTA GAG CCT TTT AGA AAA CAA AAT CCA GAC ATA G
HIV PolVif B REV B	aa aag ctt TAG CAG ATT CTG AAA AAC AAT CAA AAT AGT GCA GAT G
HIV PolVif Sequencing	GCA TTG GGA ATC ATT CAA GCA CAA CC
hAID realtime FOR	GGA CAG CCT CTT GAT GAA CCG G
hAID realtime REV	GAC CCT TAG CCC AGC GGA
β-actin realtime FOR	GCC AAC CGT GAA AAG ATG ACC C
β-actin realtime REV	CCT CGT AGA TGG GCA CAG TGT
V_λ PCR FOR	TAG CAT ATG GCG GGG CCG TCA CTG ATT GCC G
V_λ PCR REV	GCG CAA GCT TCC CCA GCC TGA CGC CAA GTC CAA G
V_λ sequencing	TTG TCT GTA AGC GGA TGC CGG

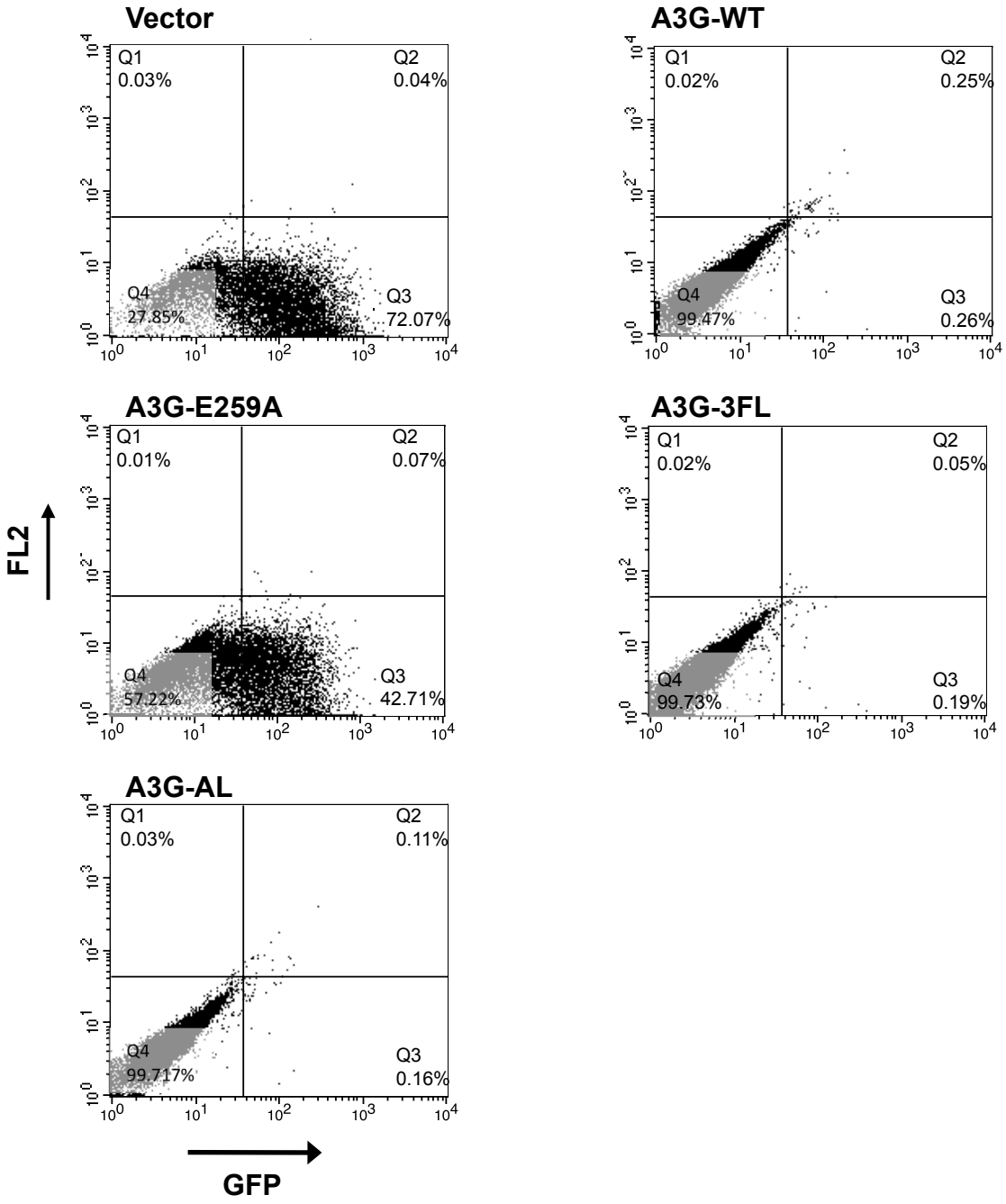

Supplemental Figure S1

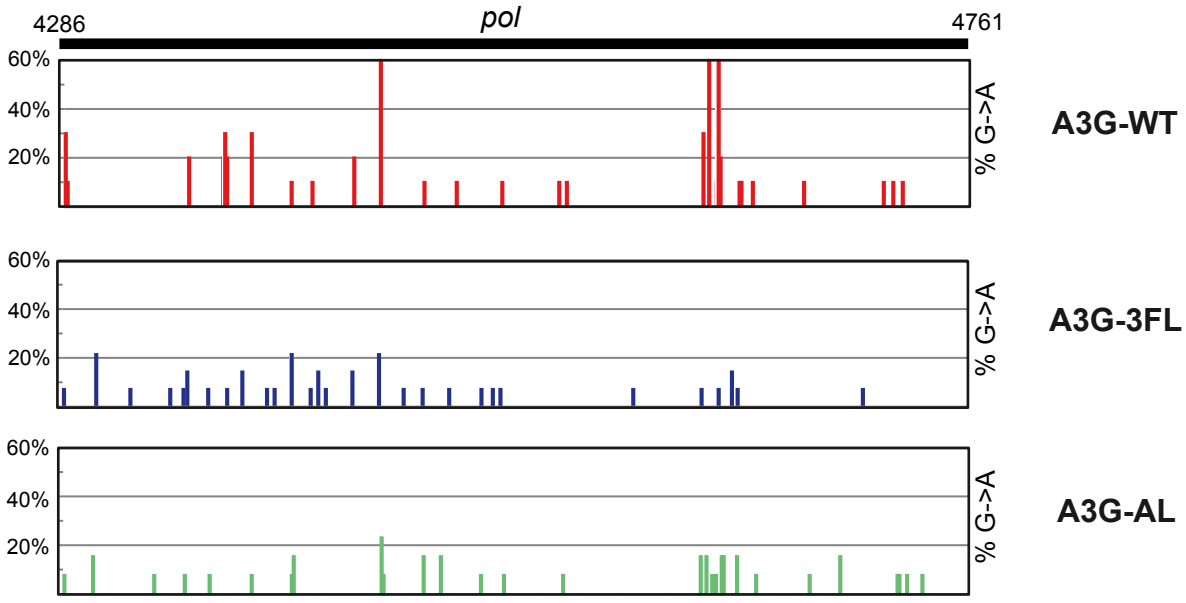

Supplemental Figure S2

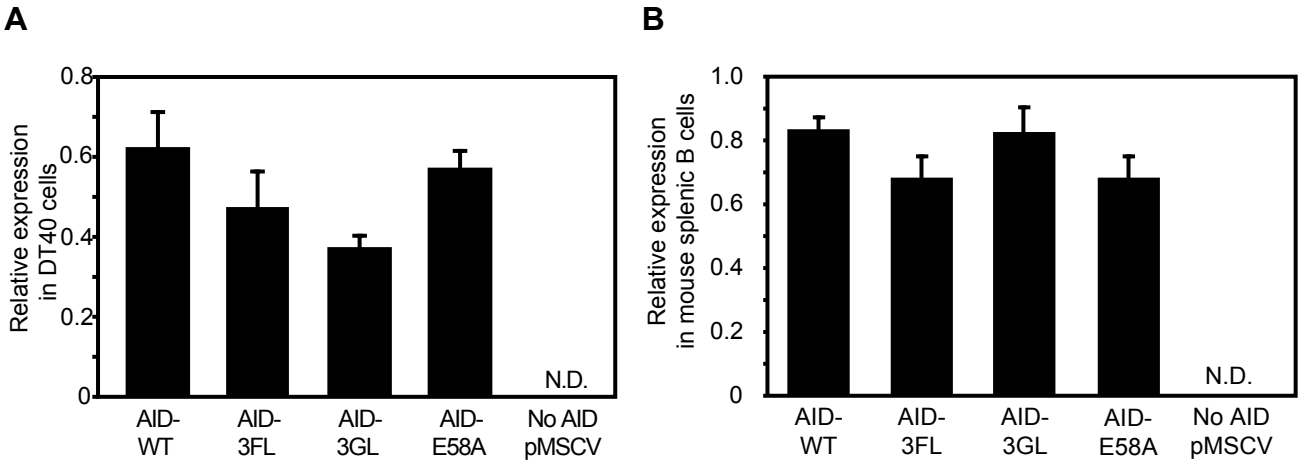

Supplemental Figure S3

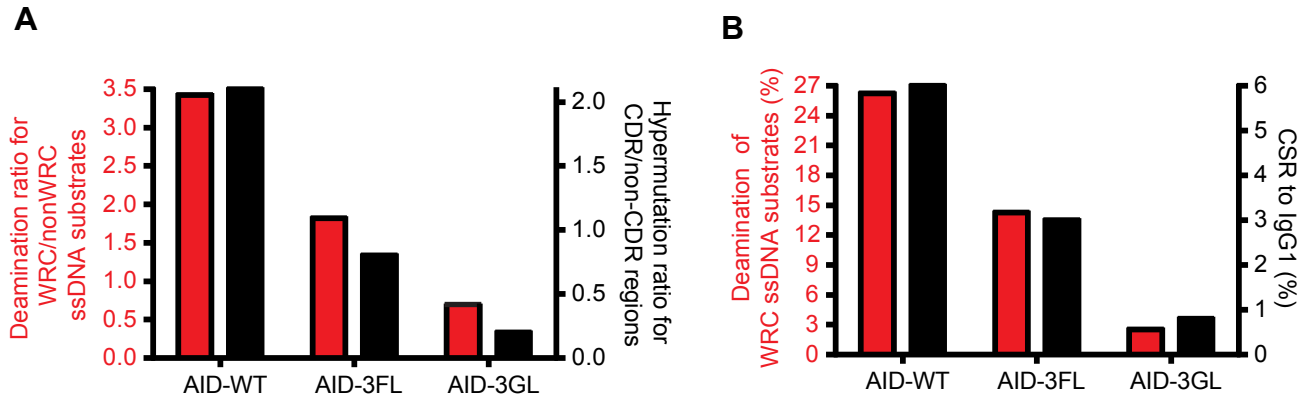

Supplemental Figure S4

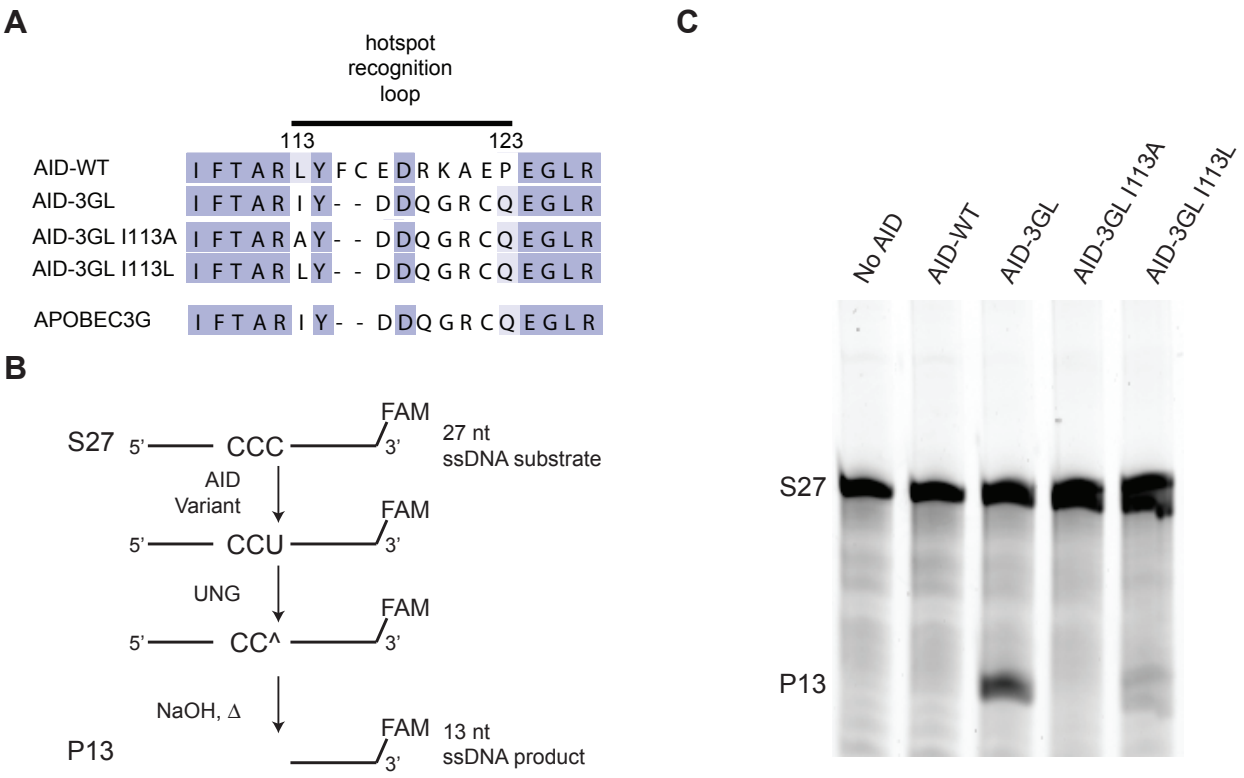

Supplemental Figure S5